J Mater Sci: Mater Electron
DOI 10.1007/s10854-016-5930-2

Chemical mechanical planarization of Al alloy in alkaline slurry at low down pressure

Yongguang Wang[1] · Yao Chen[1] · Yongwu Zhao[2] · Pengfei Min[2] · Fei Qi[1] · Xiubo Liu[1] · Dong Zhao[1]

Received: 3 September 2016 / Accepted: 20 October 2016

Abstract Effects of hydrogen peroxide and inhibitors (sodium benzoate, $NaNO_3$, sodium lauryl sulfate) on material removal at low down pressure for chemical mechanical planarization of Al alloy were investigated in alkaline slurry by using atomic force microscope, electrochemical polarization tests, Fourier transform infrared spectroscopy, and X-ray photoelectron spectroscopy. The material removal rate initially increases with concentration of H_2O_2 owing to the increase in corrosion potential and in thickness of oxidization layer, and then reaches a constant value. Additionally, surface scratch and orange peel disappear with H_2O_2. Sodium lauryl sulfate (SLS) reduces the surface roughness while maintaining a reasonable material removal rate in comparison with sodium benzoate and $NaNO_3$ due to decrease in passive current density and increase in thickness of passive layer. A weak passive layer is generated on Al alloy surface by adhesive of SLS with H_2O_2, which is easily removed at low mechanical abrasion. The chemical composition of the film layer is dominated by the Al oxide rather than sulfate though the thickness of the passive layer is increased with SLS concentration.

✉ Dong Zhao
zhaodong@suda.edu.cn

[1] School of Mechanical and Electric Engineering, Collaborative Innovation Center of Suzhou Nano Science and Technology, Soochow University, 178 East Ganjiang Road, Suzhou 215021, China

[2] School of Mechanical Engineering, Jiangnan University, Wuxi 214122, China

1 Introduction

Chemical mechanical planarization (CMP) has been widely applied as a global planarization technique in the manufacturing of ultra-large scale integrated circuits (ULSIC) [1–3]. Recently, high-k metal gate (HKMG) technique has been introduced by Intel to meet the increasing demand of the continuous shrinkage requirements in ULSIC [4, 5]. As a key integral component of the HKMG, Al CMP has been adopted by many foundries to fabricate the devices at 28 nm technology node [6–9]. During CMP, a subtle balance between mechanical abrasion and chemical erosion is crucial for the ideal Al alloy CMP process [10–12].

Previous studies were carried out to polish Al alloy in acidic media because of high removal rate and excellent corrosion protection associated with BTA as a strong inhibitor [9, 13–15]. However, the acidic process is not desirable due to the possible corrosion of the polishing equipment caused by the slurry at low pH conditions. Importantly, because of narrow dimensions and high levels of porosity at the HKMG structures, low down pressure or stress-free polishing is demanded to maintain the structural integrity [9]. As well known, the decrease in the polishing pressure leads to the reduction of polishing rate. Therefore, it is necessary to compensate the removal rate by the increase in chemical etching to maintain high removal rate.

According to the Pourbaix diagram of Al [14], aluminum alloy is etched in both acidic and alkaline media. The chemical corrosion of Al in alkaline media is more aggressive than that in acidic condition. One can infer that the alkaline polishing process could completely satisfy the above mentioned requirements and would be a promising approach to polish the Al alloy at low down pressure with high removal rate. However, the drawback of this process is that the enhancement of chemical etching usually leads

Published online: 28 October 2016

to the increase in surface roughness after Al alloy CMP [16].

Generally, the oxidize layer and passive layer generated in the CMP process play an essential role to reduce the surface damage with a reasonable material removal rate [14, 17]. H_2O_2 as an oxidizer has been frequently added to slurries to increase the electrochemical potential of Al and consequently enhances the polishing rate [18]. Hsu et al. [9] reported that a slow oxidation rate leads to excessive scratching on the surface. On the other hand, the passive etch rate on Al alloy surface should be slow enough without polishing action to avoid corrosion of metal surface. The addition of corrosion inhibitors could reduce the surface roughness effectively, which is ascribed to the formation of a complex film on the surface to reduce the isotropic etching of recessed regions on an uneven surface. For instance, HNO_3, BTA and FA/O agent were used as corrosion inhibitors to reduce the surface defect in Al CMP process due to their abilities to form complexes with Al ions [19–22].

Previous research revealed that a strong passive protection on Al alloy surface during CMP is required for high mechanical stress, leading to an excessive scratching on the surface and several damages to the HKMG. Therefore, it has yet to balance the passive corrosion at low down pressure, which requires to form a relatively weak passive film on the Al alloy surface with excellent chemical protection [23]. In spite of extensive investigations of Al CMP in acid media, effects of chemical reagents in the alkaline slurry on the material removal at low down pressure are still unclear and ambiguous. Therefore, the aim of this research is to compensate the removal rate at low down pressure by a weak passive layer in alkaline Al CMP process. Influences of hydrogen peroxide and inhibitors on the material removal were investigated and the polishing mechanism was discussed as well.

2 Experimental procedures

2.1 Materials and solutions

The experiments were carried out on rectangular samples of 7003 Al alloy panels with the dimension of 2 cm × 2 cm × 1.5 cm and the chemical composition (wt%) was: Si (0.3), Mn (0.3), Mg (0.5–1), Fe (0.35), Cu (0.2), Zn (5–6.5), Ti (0.2), Cr (0.2) and the rest Al. The samples were carefully degreased with absolute ethanol, dipped in dilute HNO_3 to remove any naturally oxidized species from the Al alloy surface, rinsed with de-ionized (DI) water, and finally dried with compressed air.

The basic polishing slurry contained DI water, dispersing agent K100 (0.2 wt%) and nano-alumina particles (purchased from Hangzhou Wanjing New Material Co. ltd., China) with a diameter of 3.5 μm at concentration of 5 wt%. The designated amounts of the oxidizer (H_2O_2) and inhibitors were added to the above basic polishing slurry. The pH of the slurry was adjusted with citric acid and tris(2-hydroxyethyl)amine. Sodium benzoate (SB), sodium lauryl sulfate (SLS) and $NaNO_3$ were used as the inhibitors, which were separately added to the basic polishing slurry in requisite amounts to achieve the desired solutions. The candidates were chosen based on the hypothesis that insoluble complexes layer could be formed on aluminium alloy surface by the effective inhibitors. The usage of all reagents was of analytical grade.

2.2 Polishing experiments

The Al alloy panels were polished for 3 min on a UNIPOL-1200S precision polisher (Shenyang Kejing Co. ltd., China) with a soft pad at down pressure of 0.6 psi, 80/80 rpm carrier/platen speed, and a slurry flow rate of 120 ml min^{-1}. Before polishing, the slurry was stirred to maintain suspension, which was continued during polishing process. The wafer weight was measured before and after polishing to calculate the weight loss and material removal rate using a precision balance (0.01 %). And each test was repeated three times to verify the reproducibility of the experimental data.

2.3 Anodic and cathodic polarization tests

Anodic and cathodic polarization tests were performed on 7003 Al panels with and without the inhibitor treatments. A CHI660E electrochemical work station with a three electrode cell was used. A commercial Ag–AgCl electrode and a platinum mesh were used as the reference and counter electrodes, respectively. An aluminum alloy encased in epoxy resin was used as the working electrode. Prior to the measurement, the aluminum alloy electrode was firstly immersed into 0.04 wt% HNO_3 for 1 min to remove the native passive films, rinsed with DI water and dried with compressed air. The exposed area was 2 cm^2. The inhibitor-treated panels were pre-immersed in the solutions for a certain period before data acquisition, i.e. 1 h, in order to achieve a steady state. The bare panels were tested immediately after exposure to the solution. On the average, three replicated samples were tested for each condition.

2.4 Surface morphology and chemical composition

Surface morphology after polishing was characterized by atomic force microscope (AFM, CSPM5000, Benyuan Co., Ltd., China) with SiN tip of a radius of 180 nm during in situ tapping model in a scanning area of 20 × 20 μm.

Fourier transform infrared (FT-IR) spectroscopy was used for structural analysis of passive film on 7003 Al alloy. The FT-IR measurements were conducted on a Nicoletis10 spectrophotometer in the mid-IR range from 4000 to 500 cm^{-1}. All the spectra were obtained at an incident angle of 75° normal to the surface of the specimens, with a spectral resolution of 0.5 cm^{-1} and the number of scans was 100.

The surface layer composition of specimens after polishing was characterized by X-ray photoelectron spectroscopy (XPS). XPS analyses were conducted with an ESCALAB 250Xi instrument, with excitation by an Al Kα radiation source (1486.6 eV) at 15 kV anode with 17 mA emission current. The binding energies were calibrated against the binding energy of C (1*s*).

3 Results and discussion

3.1 Effect of hydrogen peroxide on the polishing of Al alloy

Figure 1 shows that the material removal rate initially increases with the concentration of H_2O_2, and then reaches a constant value. The slurry used in the experiment includes the basic polishing slurry as stated in Sect. 2.1 and H_2O_2. This observation is consistent with the previously published results [18]. At low oxidizer concentration, the corrosion rate is facilitated by the addition of more oxidizer in the slurry, leading to the increase in material removal rate. However, the unreacted surface is effectively all occupied and the further increase in oxidizer content could not find any more surface molecules to react at high oxidizer concentration [12].

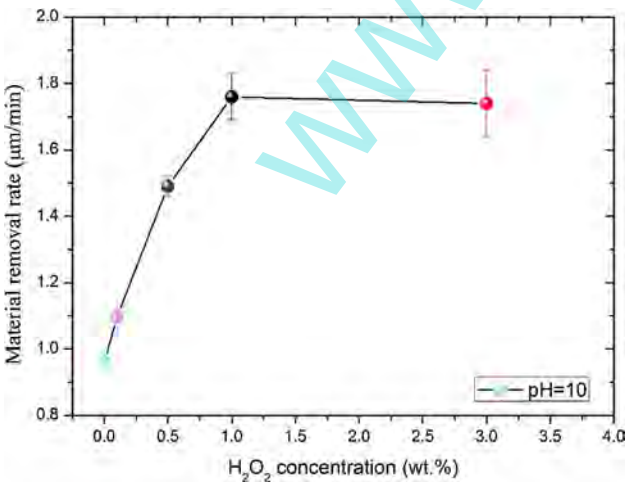

Fig. 1 Material removal rate as a function of H_2O_2 concentration

Figure 2 indicates the optical surface profiler images of the specimen after polishing with and without H_2O_2. The polishing solution is consist of the basic polishing slurry as stated in Sect. 2.1 without inhibitors. Surface damages are clearly visible in Fig. 2a without H_2O_2, such as orange peel and scratch, which could disappear with the addition of H_2O_2, as illustrated in Fig. 2b. However, the pitting corrosion as shown in Fig. 2c is observed in the presence of H_2O_2. This result strongly implies that it might be a promising approach to reduce the pitting corrosion in the polishing process by the adding of inhibitor.

3.2 Selection of the inhibitors

Previous studies revealed that inorganic salts combining with aluminium ions and organic compounds including heteroatoms (N, O, and S) are applied to retard the corrosion process of aluminium alloy in alkaline solution [24, 25]. As listed in Table 1, several inhibitor-candidates were added into the basic polishing slurry as stated in Sect. 2.1 to consider the inhibition effect and polishing results based on the hypothesis that insoluble complexes layer could be formed on aluminium alloy surface by the effective inhibitors in the presence of H_2O_2. It can be seen that surface staining occurs on the polishing specimen, though the addition of sodium tripolyphosphate prevents the corrosion of Al alloy. Therefore, sodium benzoate (SB), sodium lauryl sulfate (SLS) and $NaNO_3$ are selected as the inhibitors in the present polishing experiments.

3.3 Effect of inhibitors on the polishing of Al alloy

The comparison of the inhibition effects among SLS, SB and $NaNO_3$ on the material removal rate at pH 11 is shown in Fig. 3. Three types of solutions were used in the present experiment with the addition of the above mentioned inhibitors into the basic polishing slurry with 1 % H_2O_2. It is observed that with the increase in concentration of the inhibitors of SB and $NaNO_3$, the material removal rates are reduced due to the suppressive corrosion. It is evident from Fig. 3 that the remarkable decrease in material removal rate is followed by a slow approach to an asymptotic constant with the further increase in SLS concentration. Additionally, the sharpest decrease in the material removal rate occurs for the $NaNO_3$ compared with SLS and SB at the same concentration, implying the weaker inhibition ability of SLS and SB. The above results indicate that, with SLS as the inhibitor, higher material removal rate could easily achieve at the low down pressure of 0.6 psi. As well known, the combined interaction of passivation and mechanical abrasion is believed to be responsible for the material removal in the CMP process [11, 26]. When the rate of film formation owing to H_2O_2 and inhibitors is

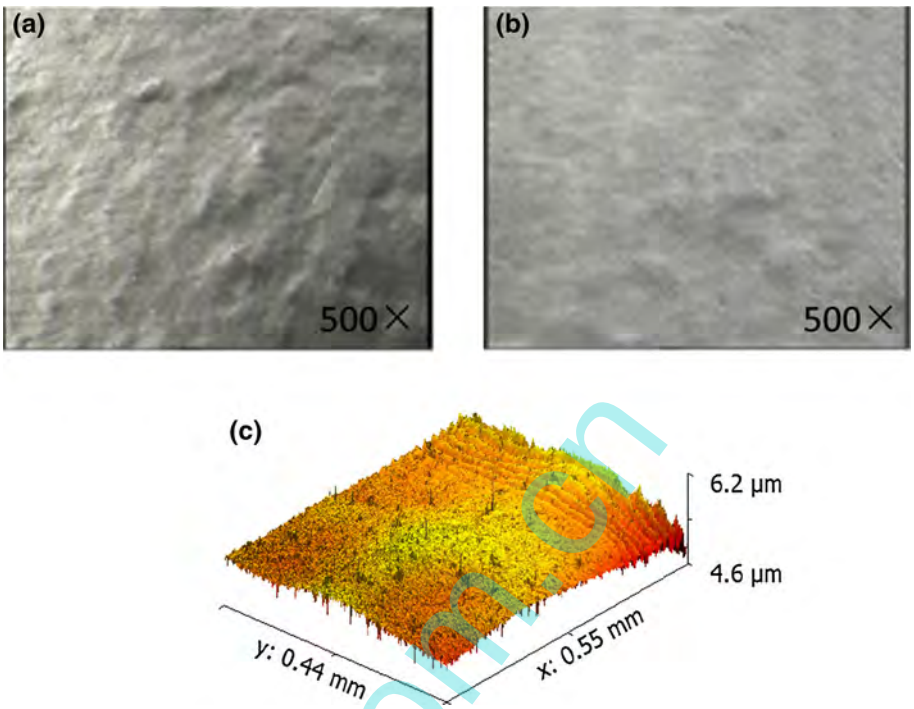

Fig. 2 Optical surface profiler images of Al alloy surface after polishing without (**a**) and with H_2O_2 (**b**) and **c** 3D image of (**b**)

Table 1 Effect of inhibitors on the inhibition effect and polishing surface

Inhibitors	Inhibition effect	Polishing surface results
Imidazole	Corrosion	–
Sodium benzoate (SB)	Non-corrosion	Bright
Sodium tripolyphosphate	Non-corrosion	Surface staining
Thiourea	Corrosion	–
Sodium gluconic	Corrosion	–
Sodium citrate	Corrosion	–
Sodium dodecyl benzene sulfate	Corrosion	–
Sodium lauryl sulfate (SLS)	Non-corrosion	Bright
$NaNO_3$	Non-corrosion	Bright
Sodium silicate	Corrosion	–
Tris(2-hydroxyethyl)amine	Corrosion	–

balanced by the rate of layer removed by the mechanical abrasion, the material removal rate is therefore maximized. This suggests that a weaker passive film is required in the case of the low down pressure polishing to obtain a higher material removal rate. For instance, at concentration of 1 %, the film formed by the $NaNO_3$ is stronger than that of SLS and SB, which might not be balanced by the mechanical abrasion at the low down pressure of 0.6 psi, leading to lower material removal rate. Interestingly, when SB % and $NaNO_3$ % are higher than ~2 %, the removal rate of the passive layer would be slower than its growth rate as shown in Fig. 3. The Al alloy CMP removal rate is dominated by the mechanical abrasion. However, when the SLS % is higher than ~2 %, the polishing rate is not further reduced as compared with SB and $NaNO_3$ (Fig. 3), implying a weaker passive layer is generated on the Al alloy surface, which subsequently leads to easy removal due to the lower mechanical abrasion.

Figure 4 shows the results of AFM surface morphologies polished by using various inhibitors as additives to the H_2O_2 -based slurries at the concentration of 1 %. It can be seen that the addition of the three inhibitors leads to significant improvement of the surface roughness compared with Ra ~500 nm for the virgin specimens without the inhibitors. Corrosion pits or scratches on the surface are hardly visible and smoother surface is obtained. Compared with SLS, SB and $NaNO_3$, SLS shows best performance in CMP process, and Ra is reduced to ~35.2 nm with the highest removal rate of 1722 nm min^{-1}, as shown in Table 2. Since the passive protection of SB and $NaNO_3$ for

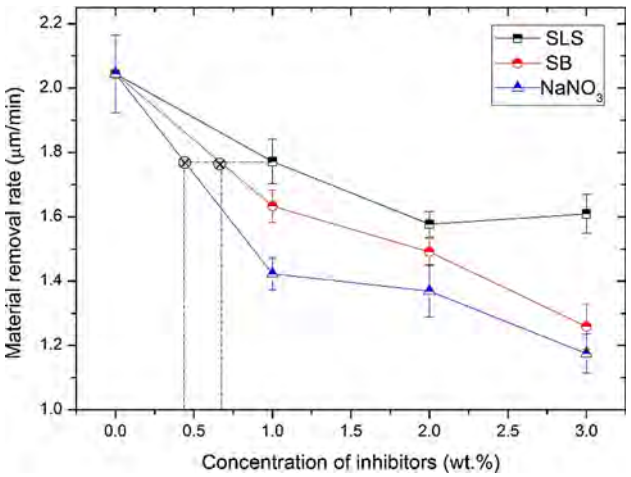

Fig. 3 Material removal rate vs. concentration of inhibitors

Al alloy surface is so strong, high mechanical stress is required to remove the passive layer in CMP process. However, the pressure at 0.6 psi is so low in the present experiment, which could not globally remove the entire passive layer generated by SB and $NaNO_3$ leading to the increase in the surface roughness. In addition, as pointed in the grey circle in Fig. 3, the less usage of the $NaNO_3$ and SB than SLS achieves the equivalent inhibition effect. Indeed, strong interaction of the inhibitor with the alloy ions in slurry could consume an amount of the inhibitor in the CMP process, leading to the decrease in the inhibitor that is applied to protect the recessed surface [23]. The impact of such consumption caused by the Al ions on a weaker inhibitor with higher concentration such as 1 % SLS is much smaller than that on a stronger one with much lower concentration (0.47 % $NaNO_3$ or 0.62 % SB). Therefore, it is concluded that SLS could achieve more stable inhibition performance than $NaNO_3$ and SB, thus achieves improved surface quality, which is confirmed by the surface roughness analysis.

Table 2 Polishing results with different inhibitors

Inhibitors	Content (wt%)	Surface roughness (Ra) (nm)	Sq (nm)
SLS	1	35.2	44.5
$NaNO_3$	1	45	57.9
SB	1	39.7	53

3.4 Effect of the oxidization layer

Figure 5 shows the effect of H_2O_2 concentration on Al alloy corrosion potential and current density. There were no abrasive particles in this test solution. Obviously, Al corrosion potential increases with the concentration of H_2O_2 owing to the formation of the oxidization layer on the

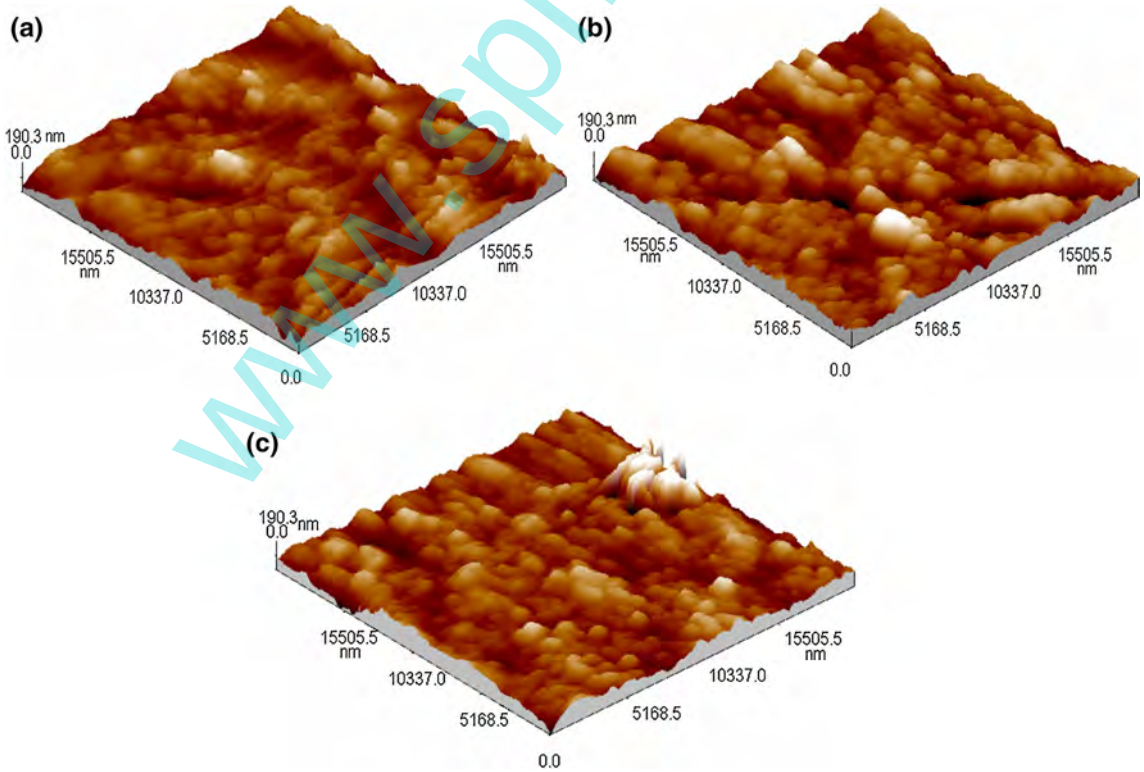

Fig. 4 The surface morphology of Al alloy after polishing with different inhibitors. **a** SLS, **b** $NaNO_3$, and **c** SB

surface of Al alloy, which hinders the anodic reaction. However, as a concentration H_2O_2 exceeds 1 %, the further increase in H_2O_2 would not sharply reduce the value of I_{corr}, inferring that additional H_2O_2 concentration has no significantly effect on the material removal rate in polishing process as shown in Fig. 1.

As described above, the formation of oxidization layer plays a significant role during CMP. XPS analysis was thus conducted to characterize the layer composition post CMP. The surface layer composition of specimens after polishing was characterized by XPS. The polishing experiment was carried out in the basic polishing slurry with SLS (1 %) and H_2O_2. Figures 6 and 7 show the spectrum of Al and S after CMP with different H_2O_2 concentrations at 1 % SLS in the polishing slurry. Binding energies of 71.89 and 74.08 eV for Al (2*p*) are assigned to the presentence of both metallic and oxidized forms of aluminum on the specimen surface, which are agreement with that reported by Kuo et al. [15]. The peak area ratio of Al^{3+} to Al^0 intensity was used to evaluate the film thickness of the residual passive layer, which technique has been proposed by Rosenbug et al. [18, 27, 28]. As shown in Fig. 8, the increase in H_2O_2 concentration leads to the increase in value of Al^{3+}/Al^0, suggesting that the thickness of the passive layer is thickened by the increase in H_2O_2 concentration. Figure 7 shows the spectrum for S(2*p*). The binding energy 168.9 eV represents the existence of SO_4^{2-}, and binding energy 170.2 eV is considered to be the presence of $AlSO_x$ due to the adhesive of SLS on the specimen surface [29, 30]. In order to explore the surface film thickness as a function of H_2O_2 content, the ratio of the peak areas of $AlSO_x$ to Al^{3+} after polishing in variable H_2O_2 concentrations are also compared in Fig. 8. A decrease in the value of $AlSO_x/Al^{3+}$ with the increasing of H_2O_2 content implies the oxidization layer comprising of an increasing amount of oxidizer rather than sulfate.

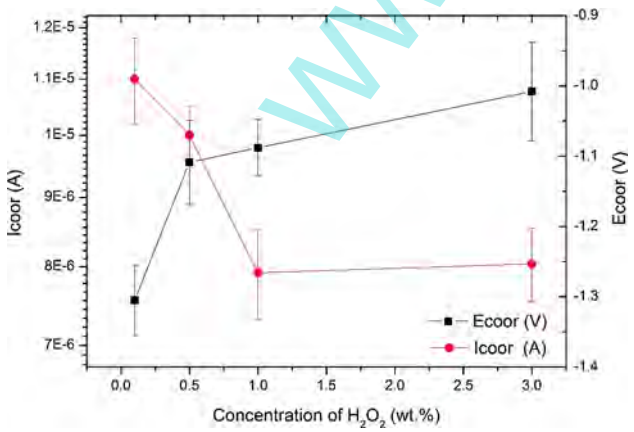

Fig. 5 I_{corr} and E_{corr} as a function of the H_2O_2 concentration

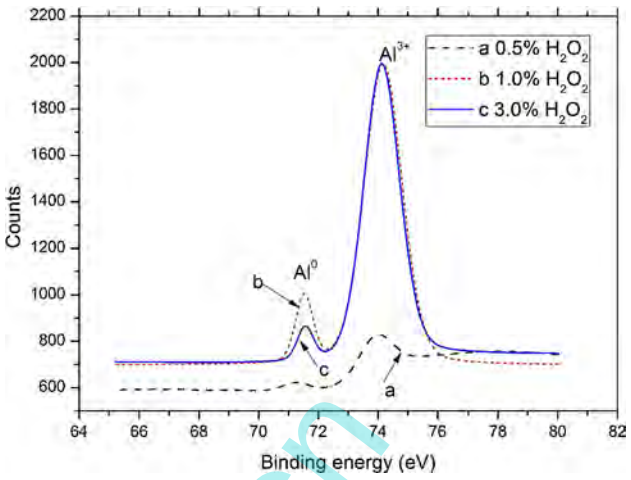

Fig. 6 XPS for Al (2*p*) spectrum after CMP of Al alloy in 1 % SLS slurry. (*a*) 0.5 % H_2O_2, (*b*) 1.0 % H_2O_2, and (*c*) 3.0 % H_2O_2

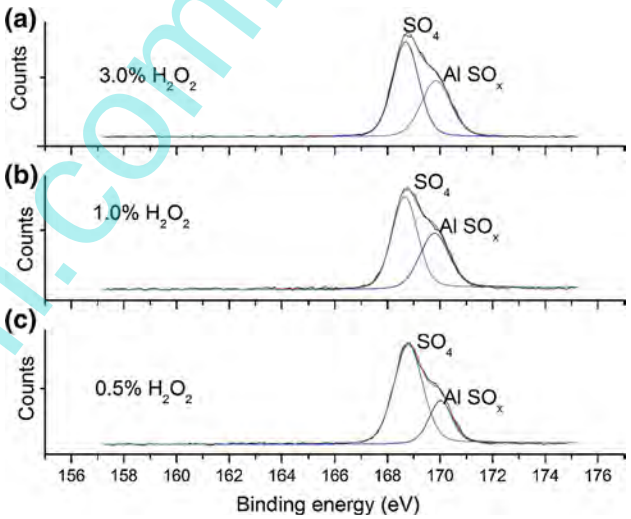

Fig. 7 XPS for S (2*p*) spectrum after CMP of Al alloy in 1 % SLS slurry. **a** 0.5 % H_2O_2, **b** 1.0 % H_2O_2, and **c** 3.0 % H_2O_2

3.5 Effect of the passive layer

The values of I_{corr} and E_{corr} of Al alloy in SLS slurry are plotted as a function of content of SLS in Fig. 9. The sample was treated in this solution without abrasive particles. E_{corr} decreases rapidly at low SLS concentration and approaches a constant at high SLS concentration, and the cathodic reaction is markedly inhibited by SLS. Additionally, an initial decrease in I_{corr} is followed by a slow approach to an asymptotic constant with the further increase in SLS concentration, which indicates that the generated film on the Al alloy surface behaves as a passive barrier.

The transmission infrared spectra of SLS-treated Al alloy is shown in Fig. 10. The strongest band near 1470 cm^{-1} is assigned to stretching of the $–CH_2$ stretching

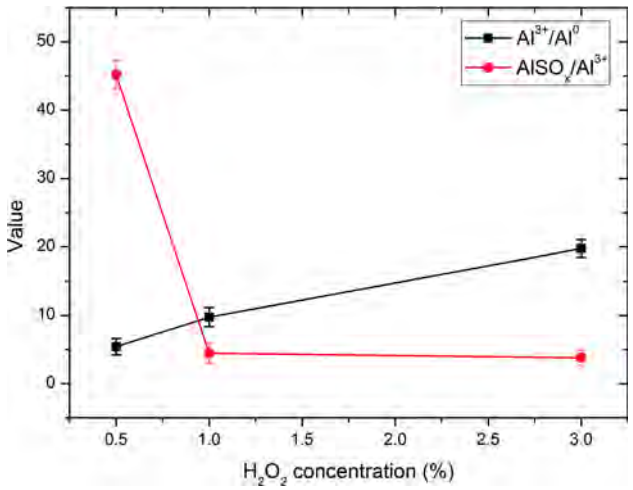

Fig. 8 Influence of H_2O_2 concentration on the changes of XPS peak area ratios of Al^{3+} to Al^0 and $Al(SO_x)$ to Al^{3+} of Al alloy in 1.0 % SLS polishing slurry

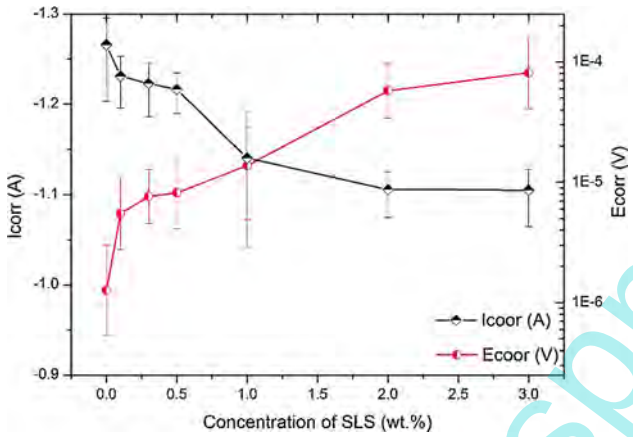

Fig. 9 I_{corr} and E_{corr} as a function of the SLS concentration

model [31]. A medium board peak centered at about 670 cm^{-1} represents the O–H wag model. A small adsorption band appears at 2898 cm^{-1} due to the methyl rocking model. The band of valence vibrations of primary OH group appears near at 3641 cm^{-1}[32]. The above mentioned characteristic absorption bands in Fig. 10 are a proof of the adhesive of SLS on the Al alloy surface, which leads to the formation of SLS-complex as a passive layer to hinder the chemical reaction. Additionally, an absorption peak owing to the Al oxide appears at 945 cm^{-1}, which is considered to be similar to Al_2O_3 on the surface [33]. This results implies that the SLS is not entirely cover the Al alloy surface.

Figure 11 shows the dependence of the S(2*p*) spectrum for the Al surface on the SLS concentration after CMP. The polishing experiment was carried out in the basic polishing slurry with H_2O_2 (1 %) and SLS. The left peak is due to the $SO4^{2-}$, whereas the right peak is owing to the adhesive of SLS on Al alloy surface.

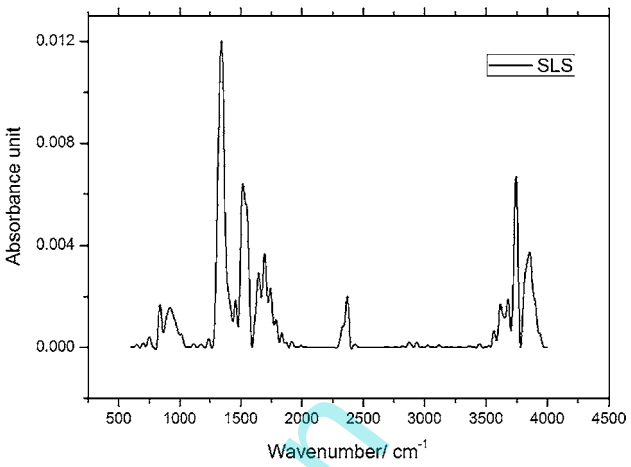

Fig. 10 FT-IR spectra of SLS treatments on Al alloy substrates

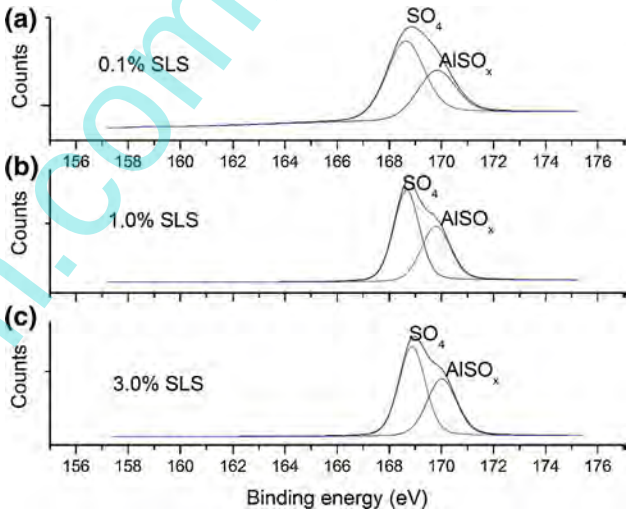

Fig. 11 XPS for S (2*p*) spectrum after CMP of Al alloy in 1 % H_2O_2 slurry. **a** 0.1 % SLS, **b** 1.0 % SLS, and **c** 3.0 % SLS

The intensity ratio of $AlSO_x$ to Al^{3+} is evaluated to calculate the film thickness of the sulfate in 1 % H_2O_2 slurry, as given in Fig. 12. It is observed that the value of $AlSO_x/Al^{3+}$ initially increases with the SLS concentration, then decreases with it. The sulfate film is thin as the concentration of SLS is low (0.1 %), and could not well protect the Al alloy surface. The further increase in the SLS leads to the decrease in value of $AlSO_x/Al^{3+}$ when the concentration of SLS exceeds 1 %, which indicates that the SLS would not form strong inhibition film on the Al alloy surface with H_2O_2. This is benefit to the polishing of Al alloy at low down pressure. It is should be pointed out that the chemical composition of the passive layer generated at 1 % SLS is dominated by the Al oxide rather than sulfate though the thickness of sulfate is increased, as confirmed from O 1*s* peak analysis in Fig. 13. The surface of the

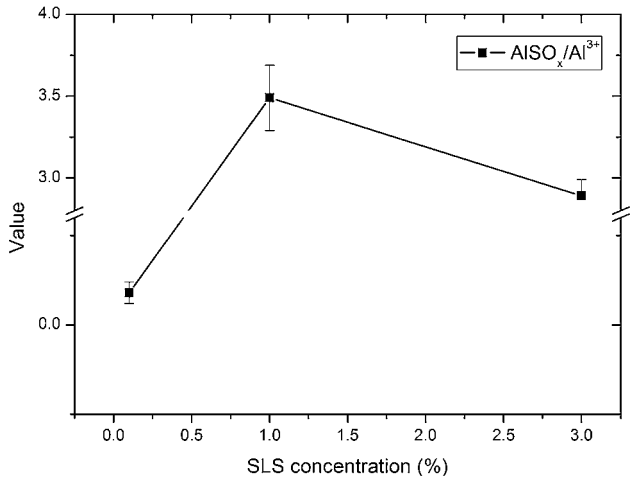

Fig. 12 Influence of H_2O_2 concentration on the changes of XPS peak area ratios of $AlSO_x$ to Al^{3+} of Al alloy in 1.0 % H_2O_2 polishing slurry

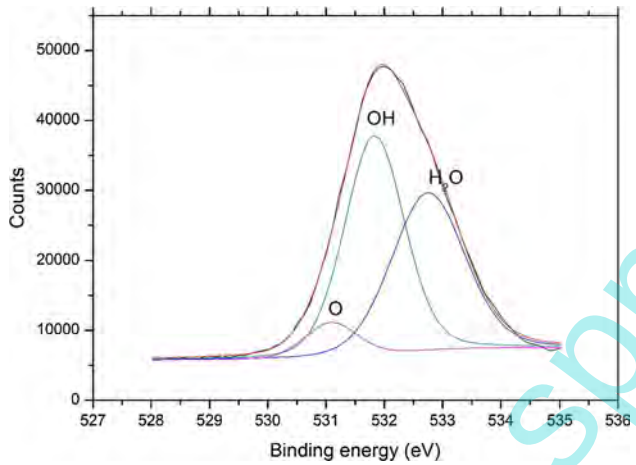

Fig. 13 XPS for O (1*s*) spectrum after CMP of Al alloy in polishing slurry with 1 % H_2O_2 and 1 % SLS

passive layer contains the hydroxyl groups with an O 1*s* binding energy of 531.8 eV and a certain of oxygen with an O 1*s* binding energy of 530.5 eV [34].

4 Conclusions

This paper studied influences of hydrogen peroxide and inhibitors on material removal in alkaline slurry for Al alloy CMP at low down pressure by using AFM, electrochemical polarization tests, FT-IR and XPS. It is found that the material removal rate initially increases with concentration of H_2O_2, and then levels off. Surface scratch and orange peel disappear with H_2O_2. SLS reduces the surface roughness while maintaining a reasonable material removal rate in comparison with sodium benzoate and $NaNO_3$, which indicates that a weak passive layer is generated on the Al alloy surface being easily removed at low mechanical abrasion. The electrochemical behavior of Al alloy in the alkaline slurry is markedly modified by hydrogen peroxide and SLS to enhance the corrosion potential and to reduce the passive current density, respectively. XPS examinations suggest that the thicknesses of oxidization layer and passive layer are enhanced with concentrations of hydrogen peroxide and SLS. However, the chemical composition of the film layer is dominated by the Al oxide rather than sulfate.

Acknowledgments This research work was financially supported by National Natural Science Foundation of China (Grant Numbers: 11402156, 51471113, 51275326, U1533101, and 51501121), China Postdoctoral Science Foundation (Grant Number: 2015M571800), Jiangsu Postdoctoral Science Foundation (Grant Number: 1402121C).

References

1. H. Lee, D. Lee, H. Jeong, Mechanical aspects of the chemical mechanical polishing process: a review. Int. J. Precis. Eng. Manuf. **17**, 525–536 (2016)
2. Y. Chen, J. Qin, Y. Wang, Z. Li, Core/shell composites with polystyrene cores and meso-silica shells as abrasives for improved chemical mechanical polishing behavior. J. Nanopart. Res. **17**, 1–11 (2015)
3. Y. Chen, Y. Wang, J. Qin, A. Chen, Core/shell structured solid-silica/mesoporous-silica microspheres as novel abrasives for chemical mechanical polishing. Tribol. Lett. **58**, 1–8 (2015)
4. H.K. Sung, C. Wang, N.Y. Kim, Ultra-smooth $BaTiO_3$ surface morphology using chemical mechanical polishing technique for high-k metal-insulator-metal capacitors. Mater. Sci. Semicon. Proc. **40**, 516–522 (2015)
5. U.R.K. Lagudu, A.M. Chockalingam, S.V. Babu, Chemical mechanical polishing of Al-Co films for replacement metal gate applications. J. Solid State Sci. **2**, Q77–Q82 (2013)
6. Q. Xu, L. Chen, A material removal rate model for aluminum gate chemical mechanical planarization. J. Solid State Sci. **4**, P101–P107 (2015)
7. Q. Xu, L. Chen, J. Fang, F. Yang, A chemical mechanical planarization model for aluminum gate structures. Microelectron. Eng. **131**, 58–67 (2015)
8. Q. Xu, L. Chen, An aluminum gate chemical mechanical planarization model for HKMG process incorporating chemical and mechanical effects. J. Solid State Sci. **3**, P60–P74 (2014)
9. H.K. Hsu, T.C. Tsai, C.W. Hsu, W. Lin, R.P. Huang, C.L. Yang, J.Y. Wu, Defect reduction of replacement metal gate aluminum chemical mechanical planarization at 28 nm technology node. Microelectron. Eng. **112**, 121–125 (2013)
10. Y. Wang, Y. Chen, F. Qi, D. Zhao, W. Liu, A material removal model for silicon oxide layers in chemical mechanical planarization considering the promoted chemical reaction by the down pressure. Tribol. Int. **93**, 11–16 (2016)
11. L.M. Nolan, K.C. Cadien, Chemically enhanced synergistic wear: a copper chemical mechanical polishing case study. Wear **307**, 155–163 (2013)
12. Y. Wang, Y. Zhao, J. Jiang, X. Li, J. Bai, Modeling effect of chemical-mechanical synergy on material removal at molecular scale in chemical mechanical polishing. Wear **265**, 721–728 (2008)

13. X. Shi, S.E. Rock, M.C. Turk, D. Roy, Minimizing the effects of galvanic corrosion during chemical mechanical planarization of aluminum in moderately acidic slurry solutions. Mater. Chem. Phys. **136**, 1027–1037 (2012)
14. Y.L. Wang, W.T. Tseng, S.C. Chang, Chemical-mechanical polish of aluminum alloy thin films: slurry chemistries and polish mechanisms. Thin Solid Films **474**, 36–43 (2005)
15. H.S. Kuo, W.T. Tsai, Electrochemical behavior of aluminum during chemical mechanical polishing in phosphoric acid base slurry. J. Electrochem. Soc. **147**, 149–154 (2000)
16. Q. Luo, D.R. Campbell, S.V. Babu, Chemical-mechanical polishing of copper in alkaline media. Thin Solid Films **311**, 177–182 (1997)
17. J. Hernandez, P. Wrschka, Y. Hsu, T.S. Kuan, G.S. Oehrlein, H.J. Sun, D.A. Hansen, J. King, M.A. Fury, Chemical mechanical polishing of Al and SiO_2 thin films: the role of consumables. J. Electrochem. Soc. **146**, 4647–4653 (1999)
18. H.S. Kuo, W.T. Tsai, Effects of alumina and hydrogen peroxide on the chemical-mechanical polishing of aluminum in phosphoric acid base slurry. Mater. Chem. Phys. **69**, 53–61 (2001)
19. T.H. Tsai, Y.F. Wu, S.C. Yen, Glycolic acid in hydrogen peroxide-based slurry for enhancing copper chemical mechanical polishing. Microelectron. Eng. **77**, 193–203 (2005)
20. M. Ronay, Development of aluminum chemical mechanical planarization. J. Electrochem. Soc. **148**, G494–G499 (2001)
21. C.G. Kallingal, D.J. Duquette, S.P. Murarka, An investigation of slurry chemistry used in chemical mechanical planarization of aluminum. J. Electrochem. Soc. **145**, 2074–2081 (1998)
22. X. Luan, Y. Liu, C. Wang, G. Liu, Stability of weakly alkaline barrier slurry with the high selectivity. Microelectron. Eng. **130**, 28–34 (2014)
23. L. Jiang, Y. Lan, Y. He, Y. Li, Y. Li, J. Luo, 1,2,4-Triazole as a corrosion inhibitor in copper chemical mechanical polishing. Thin Solid Films **556**, 395–404 (2014)
24. M.G. Mahjani, M. Sabzali, M. Jafarian, J. Neshati, An investigation of the effects of inorganic inhibitors on the corrosion rate of aluminum alloy using electrochemical noise measurements and electrochemical impedance spectroscopy. Anti-Corros. Method. Mater. **55**, 208–216 (2008)
25. S.V. Lamaka, M.L. Zheludkevich, K.A. Yasakau, M.F. Montemor, M.G.S. Ferreira, High effective organic corrosion inhibitors for 2024 aluminium alloy. Electrochim. Acta **52**, 7231–7247 (2007)
26. J. Li, Y. Liu, X. Lu, J. Luo, Y. Dai, Material removal mechanism of copper CMP from a chemical–mechanical synergy perspective. Tribol. Lett. **49**, 11–19 (2013)
27. P. Wrschka, J. Hernandez, Y. Hsu, T.S. Kuan, G.S. Oehrlein, H.J. Sun, D.A. Hansen, J. King, M.A. Fury, Polishing parameter dependencies and surface oxidation of chemical mechanical polishing of Al thin films. J. Electrochem. Soc. **146**, 2689–2696 (1999)
28. R.A. Rosenberg, M.W. Mcdowell, J.R. Noonan, X-ray photoelectron spectroscopy analysis of aluminum and copper cleaning procedures for the advanced photon source. J. Vac. Sci. Technol., A **12**, 1755–1759 (1994)
29. C. Petit, M. Seredych, T.J. Bandosz, Revisiting the chemistry of graphite oxides and its effect on ammonia adsorption. J. Mater. Chem. **19**, 9176–9185 (2009)
30. F.C. Galisteo, C. Larese, R. Mariscal, M.L. Granados, J. Fierro, R. Fernandez-Ruiz, M. Furio, Deactivation on vehicle-aged diesel oxidation catalysts. Top. Catal. **30**, 451–456 (2004)
31. P. Selvakumar, B.B. Karthik, C. Thangavelu, Surface and electrochemical characterization of corrosion inhibition of stainless steel in acid medium. J. Mater. Environ. Sci. **6**, 1750–1757 (2014)
32. S. Rajendran, K. Anuradha, K. Kavipriya, A. Krishnaveni, J. Jeyasundari, V. Sribharathy, Inhibition of corrosion of carbon steel in sea water by sodium gluconate-Zn^{2+} system. Port. Electrochim. Acta. **31**, 141–155 (2013)
33. H. Ogawa, Y. Tokuyama, M. Yanagisawa, H. Nakagawa, J. Kikuchi, Y. Horiike, Study on the mechanisms of chemical mechanical polishing on copper and aluminum surfaces employing in situ infrared spectroscopy. Jpn. J. Appl. Phys. **42**, 3582–3587 (2003)
34. J.T. Kloprogge, L.V. Duong, B.J. Wood, R.L. Frost, XPS study of the major minerals in bauxite: Gibbsite, bayerite and (pseudo-)boehmite. J. Colloid Interf. Sci. **296**, 572–576 (2006)